Evaluation of the effectiveness of current guidelines in determining the strength of RC beams retrofitted by means of NSM reinforcement

T. D'Antino *, M.A. Pisani

Department of Architecture, Built Environment, and Construction Engineering, Politecnico di Milano, Italy

Near surface mounted (NSM) fiber reinforced polymer (FRP) reinforcement represents a valid alternative to externally bonded (EB) FRP reinforcement for strengthening existing reinforced concrete (RC) elements. NSM composites are usually comprised of glass, carbon, and aramid fiber reinforcement with circular (bars) or prismatic (strips) cross-section. When the NSM technique is employed for flexural strengthening, FRP composites are embedded into grooves cut in the concrete cover and filled with an inorganic (e.g. cement grout) or organic (e.g. epoxy resin) binding agent. Although many studies on the bond behavior of NSM FRP composites can be found in the literature, limited work is available regard-ing analytical models for designing NSM strengthening of RC members. In this paper, a database com-prised of 155 experimental tests on RC beams strengthened in flexure using NSM reinforcement is collected from the scientific literature. The experimental database is employed to assess the accuracy of the analytical provisions obtained following the American, English, Canadian, and Italian guidelines. The assessment shows that, although conservative, the analytical models considered are (relatively) poorly accurate and further studies are needed to provide a reliable tool for designing RC flexural strengthening with NSM reinforcement.

Keywords: NSM, RC beams, Strengthening ,Analytical formulation ,Assessment

1. Introduction

In the last decades, fiber reinforced composite materials have gained increasing popularity in the civil engineering industry. Among them, fiber reinforced polymer (FRP) composites have been employed to strengthen existing reinforced concrete (RC) and masonry elements. FRP composite strips are largely applied to existing elements as externally bonded (EB) reinforcement (see e.g. [1]). A valid alternative to EB FRP systems is represented by near surface mounted (NSM) FRP systems. In the NSM method, grooves are first cut into the concrete cover of an RC element and the added reinforcement is bonded therein with an appropriate groove filler (typically epoxy paste or cement grout) [2].

The first applications of the EBR technique, made with steel plates, are half a century old [3–5]. Before that, strengthening made by means of near-surface mounted (NSM) steel rebar had already been adopted in practice [6]. However, the NSM method had a limited success with respect to externally bonded reinforcement applications. One of the main reasons why externally bonded reinforcement was preferred to near-surface mounted lies in the possibility to increase the steel plate-to-concrete bond by means of bolts (adequately anchored into the concrete substrate) placed along the length of the plate – usually along the anchorage length – to avoid debonding failures. This solution guarantees the effectiveness of the external reinforcement, which in turn allows for attaining concrete crushing failure.

EBR systems made with steel plates is an effective solution but suffers of some disadvantages, among which the problem of corrosion of the steel plates and the difficulty in manipulating heavy and long plates in construction sites are the most important. Replacing the steel plates with fiber reinforced polymer (FRP) sheets provides a satisfactory solution to the problems described above and, because of this, has been increasingly studied an adopted starting from the eighties of the last century [7]. Nevertheless, the adoption of FRP (mainly carbon fiber reinforced polymer, or CFRP) sheets does not generally allow for using anchor bolts because of the mechanical properties of the composite sheet. This fact implies that the efficiency of an externally bonded FRP reinforcement is limited by the delamination of the composite, which can be related either to debonding of the sheet from the substrate with a relatively thin layer of concrete attached to it or to splitting of the entire concrete cover at the level of the tensile reinforcement [1].

More recently, near-surface mounted (NSM) FRP reinforcement has attracted an increasing amount of research as well as practical

Article history:
Received 18 August 2016
Revised 10 January 2017
Accepted 28 January 2017
Available online 2 February 2017

* Corresponding author.
E-mail address: tommaso.dantino@polimi.it (T. D'Antino).

© 2017. This manuscript version is made available under the CC-BY-NC-ND 4.0 license http://creativecommons.org/licenses/by-nc-nd/4.0/
Published Journal Article available at http://dx.doi.org/10.1016/j.compstruct.2017.01.070

application. NSM systems were proved to be more efficient than EBR systems because the NSM strips are less sensitive to debonding phenomena (see for instance [2,8,9]). Although NSM reinforcement cannot be used in concrete elements for which the cover depth is low, NSM bars are protected by the concrete cover and are less exposed to accidental impacts, mechanical damage, fire, and vandalism and the aesthetic aspect of the strengthened structure is virtually unchanged [10].

Extensive research has been carried out to investigate the NSM-concrete bond behavior (see for instance [11–15]). However, limited work is available regarding analytical models for designing NSM strengthening of RC members.

In this paper, three analytical models for the estimation of the bending capacity of RC beams strengthened with NSM FRP composites (i.e. American ACI 440.2R-08 [2], English TR 55 [16], and Canadian CSA S806-12 guidelines [17]) are analyzed. Furthermore, the procedure for EB reinforcement proposed by the Italian CNR-DT 200 R1/2013 [1] is extended to the case of NSM reinforcement. An experimental database comprised of 155 RC beams strengthened in flexure with NSM reinforcement was collected from the literature. Comparisons between the maximum bending moment computed by the analytical models and the corresponding experimentally measured value allowed to assess the accuracy of each model.

2. NSM flexural strengthening analytical models

The accuracy of the analytical methods proposed by the American ACI 440.2R-08 [2], English TR 55 [16], and Canadian CSA S806-12 [17] guidelines for the evaluation of the flexural capacity of NSM strengthened RC members was assessed in this paper. In addition, the procedure included in the Italian guideline CNR-DT 200 R1/2013 [1] for the evaluation of the flexural capacity of EB FRP strengthened RC members was extended to the case of NSM reinforcement and its accuracy was assessed using the experimental database collected.

All analytical models considered in this paper have a solid fracture mechanics framework. The maximum strain of a near surface mounted FRP bar should be computed by evaluating the fracture energy of the specific interface where fracture is assumed to occur. However, since the evaluation of the fracture energy associated with each possible fracture interface is a difficult task, simplified formulations are adopted by design codes/recommendations.

All procedures considered are based on the assumptions that plane sections remain plane, there is no relative slip between FRP reinforcement and concrete, and FRP reinforcement has a linear-elastic stress-strain behavior up to failure. These assumptions, although questionable, appear to be reasonable for design purposes and their validity can be confirmed by comparison between experimental results and corresponding analytical provisions. Failure of the strengthened member is assumed when one of the following scenarios occurs:

i. failure (rupture or debonding) of the NSM reinforcement, which is assumed to occur when the strain in the NSM reinforcement attains the maximum value ε_{fd};
ii. concrete crushing, which is assumed to occur when the concrete strain is equal to 0.003 in the case of American guideline, and to 0.0035 in the remaining guidelines considered;
iii. simultaneous rupture of NSM reinforcement and crushing of concrete, referred to as *balanced failure* in the Canadian guideline [17].

The analytical formulations provided by each guideline for computing the maximum NSM strain ε_{fd} are here briefly recalled for the sake of clarity. Wherever possible, the same notation employed in the original documents was adopted.

2.1. ACI 440.2R-08 [2]

According to the American guideline ACI 440.2R-08 [2] the maximum strain in the FRP reinforcement is affected by many factors (e.g. the member dimensions, reinforcement ratio, and treatment of the FRP reinforcement surface) and is included within the range $0.6\varepsilon_{fu}$ and $0.9\varepsilon_{fu}$, where ε_{fu} is the design rupture strain of the FRP reinforcement:

$$\varepsilon_{fu} = C_E \cdot \varepsilon^*_{fu} \tag{1}$$

where ε^*_{fu} is the ultimate rupture strain of the FRP reinforcement and C_E is an environmental reduction factor, which was assumed equal to 1.0 in this study. C_E accounts for the possible reduction of the composite properties due to the exposition of the strengthening system to certain environmental conditions for a relatively long time. The environmental reduction factor C_E was assumed equal to 1.0 in this paper because the environmental conditions during laboratory tests are controlled and no reduction of the composite properties due to environmental exposure should occur. The maximum value of the strain in the FRP reinforcement is recommended to be:

$$\varepsilon_{fd} = 0.7\varepsilon_{fu} \tag{2}$$

In order to achieve ε_{fd} the FRP reinforcement should have a bonded length greater than the development length l_{db}, which is defined as the length needed to achieve the design strength [2]:

$$l_{db} = \frac{d_b}{4\tau_b} f_{fd} \quad \text{for circular bars} \tag{3}$$

$$l_{db} = \frac{a_b \cdot b_b}{2(a_b + b_b)\tau_b} f_{fd} \quad \text{for rectangular bars} \tag{4}$$

where d_b is the diameter of the NSM bar, τ_b is the average bond strength, which is assumed equal to 6.9 MPa, f_{fd} is the design strength of the NSM reinforcement, and a_b and b_b are the width and thickness of the NSM plate, respectively.

2.2. TR 55 [16]

According to the English guideline TR 55 [16], NSM strengthening of RC beams should be designed against three different failure modes, namely concrete cover separation, concrete splitting failure, and failure in the adhesive layer. To avoid concrete cover separation, the strain in the FRP should be limited to:

$$\varepsilon_{lim} = 38\sqrt{\frac{b}{n} \cdot \frac{f_{ctk}}{E_f A_f}} \leqslant \varepsilon_{fu} \tag{5}$$

where b is the width of the concrete cross-section, n is the number of NSM bars employed, f_{ctk} is the concrete characteristic tensile strength, E_f is the FRP modulus of elasticity, and A_f is the area of the single NSM bar.

To avoid concrete splitting failure the strain in the FRP reinforcement in the cross-section where the FRP is needed, i.e. where yielding of the steel reinforcement starts to occur, should be limited to the maximum ultimate anchorage strain ε_{max}:

$$\varepsilon_{max} = \begin{cases} 10 \cdot b_{notchperim}\sqrt{\frac{f_{ctk}}{E_f A_f}} & \text{for } l \geqslant l_{db} \\ 10 \cdot b_{notchperim}\sqrt{\frac{f_{ctk}}{E_f A_f}} \cdot \frac{l}{l_{db}}\left(2 - \frac{l}{l_{db}}\right) & \text{for } l < l_{db} \end{cases} \tag{6}$$

where $b_{notchperim}$ is the effective perimeter of notch, which is generally assumed as the minimum depth plus the minimum width if no special methods were employed to prepare the notch sides, l is the

NSM reinforcement anchorage length, and l_{db} is the development length (referred to as anchorage length l_{max} in TR 55 [16]):

$$l_{db} = l_{max} = 0.135 \cdot b_{notchperim} \sqrt{\frac{E_f A_f}{f_{ctk}}} \tag{7}$$

To prevent failure in the adhesive layer, the strain in the NSM reinforcement should be limited to:

$$\varepsilon_{ad} = \frac{0.3 \cdot f_{at} \cdot b_{barperim} \cdot l}{E_f A_f} \tag{8}$$

where f_{at} is the adhesive tensile strength and $b_{barperim}$ is the perimeter of the NSM bar. The maximum strain ε_{fd} in the NSM reinforcement is:

$$\varepsilon_{fd} = \min\{\varepsilon_{lim}, \varepsilon_{max}, \varepsilon_{ad}\} \tag{9}$$

As a first attempt to assess the accuracy of the analytical procedure proposed for computing the maximum strain ε_{fd}, the shear stresses at the adhesive-concrete and adhesive-NSM reinforcement interfaces were assumed to be lower than the corresponding maximum values allowed, i.e. separation failure is prevented [16].

2.3. CSA S806-12 [17]

The Canadian standard CSA S806-12 [17] does not provide specific formulations to prevent FRP debonding failure. However, the maximum strain in the NSM reinforcement is limited to 0.007 and limitations on the mechanical properties of the FRP composite are enforced. Therefore, according to the Canadian formulation, failure of an NSM flexural strengthened RC beam occurs either when the concrete strain is equal to 0.003 (i.e. concrete crushing) and the strain in the NSM reinforcement is lower or equal to 0.007, or when the strain in the NSM reinforcement is ε_{fd} = 0.007 and the concrete strain is lower or equal to 0.003. When the strain in the concrete and NSM reinforcement is simultaneously equal to 0.003 and 0.007, respectively, balanced failure occurs.

2.4. CNR-DT 200 R1/2013 [1]

The Italian guideline CNR-DT 200 R1/2013 [1] provides accurate design procedures for strengthening existing structural members with EB FRP composites [18,19]. A specific procedure for designing NSM strengthening is not provided. As a first attempt to propose a design approach based on the Italian guideline procedure, the analytical approach provided by CNR-DT 200 R1/2013 [1] for EB reinforcement was extended to the case of NSM reinforcement. The same procedure and hypotheses proposed for EB reinforcement were employed for the case of NSM reinforcement. To take into account the different geometry of NSM reinforcement with respect to EB reinforcement, the thickness t_f and width b_f of an EB FRP strip were related to the geometrical properties of the NSM reinforcement as follows:

$$b_f = \begin{cases} \frac{\pi \cdot d_n}{2} n & \text{for circular bars} \\ (b_n + 2h_n) \cdot n & \text{for rectangular bars} \end{cases} \tag{10}$$

$$t_f = \begin{cases} \frac{\pi \cdot d_n^2}{4} \frac{n}{b_f} & \text{for circular bars} \\ \frac{b_n \cdot h_n \cdot n}{b_f} & \text{for rectangular bars} \end{cases} \tag{11}$$

where d_n is the diameter of the nth NSM circular bar, and b_n and h_n are the width and thickness of the nth NSM rectangular bar, respectively. By using Eqs. (10) and (11) it is possible to employ the analytical approach for EB reinforcement proposed by the Italian guidelines to estimate the flexural capacity of NSM strengthened RC beams as follows. According to the Italian guideline, the strain in the FRP reinforcement should be limited to ε_{fd}:

$$\varepsilon_{fd} = \min\left\{\frac{\eta_a \cdot \varepsilon_{fk}}{\gamma_f}, \varepsilon_{fdd}\right\} \tag{12}$$

where η_a is an environmental conversion factor (assumed equal to 1.0 in this study), γ_f is a material safety factor (assumed equal to 1.0 in this study), ε_{fk} is the FRP characteristic failure strain, and ε_{fdd} is the FRP intermediate crack-induced (IC) debonding strain:

$$\varepsilon_{fdd} = \frac{k_q}{\gamma_{f,d}} \sqrt{\frac{2 \cdot k_b \cdot k_{G,2}}{t_f E_f \cdot FC} \sqrt{f_{cm} \cdot f_{ctm}}} \tag{13}$$

where k_q = 1.25 for distributed loads and k_q = 1.00 otherwise, $\gamma_{f,d}$ is a safety factor that depends on the probability associated with debonding failure (assumed equal to 1.0 in this study), FC is a confidence factor that depends on the level of knowledge of the element to be strengthened (assumed equal to 1.0 in this study), $k_{G,2}$ is a corrective factor with a calibrated mean value of 0.32 mm, f_{cm} and f_{ctm} are the concrete mean compressive and tensile strength, respectively, and k_b is a geometrical corrective factor:

$$k_b = \sqrt{\frac{2 - b_f/b}{1 + b_f/b}} \geqslant 1 \text{ for } b_f/b \geqslant 0.25 \tag{14}$$

To prevent plate-end (PE) debonding failure, the strain in the FRP reinforcement in the cross-section where yielding of the steel reinforcement starts to occur under the applied load of the strengthened configuration, should be limited to:

$$\varepsilon_{fdd} = \begin{cases} \frac{1}{\gamma_{f,d}} \sqrt{\frac{2 \cdot k_b \cdot k_G}{t_f E_f \cdot FC} \sqrt{f_{cm} \cdot f_{ctm}}} & \text{for } l \geqslant l_{db} \\ \frac{1}{\gamma_{f,d}} \sqrt{\frac{2 \cdot k_b \cdot k_G}{t_f E_f \cdot FC} \sqrt{f_{cm} \cdot f_{ctm}}} \cdot \frac{l}{l_{db}} \left(2 - \frac{l}{l_{db}}\right) & \text{for } l < l_{db} \end{cases} \tag{15}$$

where the development length l_{db} (referred to as optimal bond length l_{ed} in CNR-DT 200 R1/2013 [1]) is:

$$l_{db} = l_{ed} = \min\left\{\frac{1}{\gamma_{Rd}} \sqrt{\frac{\pi^2 \cdot t_f E_f \cdot s_u^2 \cdot FC}{8 \cdot k_b k_G \sqrt{f_{cm} \cdot f_{ctm}}}},\ 200 \text{ mm}\right\} \tag{16}$$

where k_G is a geometrical corrective factor with a calibrated mean value of 0.063 mm (for pre-cured FRP composites, as in the case of NSM reinforcement), and s_u = 0.25 mm is the FRP-concrete interfacial debonding slip.

3. Experimental database

An experimental database comprised of 155 RC beams strengthened in flexure using NSM reinforcement was collected from the literature. The database includes experimental tests of 114 rectangular beams and 41 T-beams carried out from 28 different working groups [9,14,20–45]. The main characteristics of the specimens collected are listed in Table 1. Specimens in Table 1 are labeled with the same name adopted by the authors of the tests. The frequency distribution of specimens included in the database is depicted in Fig. 1 for different ranges of geometrical and mechanical properties considered.

The ratio between the beam span l_s and corresponding effective cross-section depth d varies between 6.3 and 19.6 (Fig. 1a), with 43.2% of the specimens having l_s/d = 9–11.6. Although the concrete mean compressive strength f_{cm} (Fig. 1b) varies between 15.0 MPa and 67.2 MPa, 65.2% of the specimens have an f_{cm} higher than 35.9 MPa, which is not representative of old reinforced concrete elements in need of strengthening. The tensile steel reinforcement mechanical ratio ρ_s (Fig. 1c) is:

$$\rho_s = \frac{A_s f_y}{A_c f_{cm}} \tag{17}$$

Table 1
Database of NSM strengthened RC beams collected from the literature.

Name		Cross-section				Mechanical properties			NSM composite					Exp results		Analytical M_{th} [kNm]			
		S	b_w [mm]	a/d	l/d	f_{cm} [MPa]	f_{sy} [MPa]	ρ_s	F	f_{fk} [MPa]	E_f [GPa]	B	$\rho\rho_f$	M_{exp} [kNm]	FM	[2]	[16]	[17]	[1]
[9]	NSM_c_2x1.4x10_1	R	120	8.41	19.09	17.4	540	0.253	C	2052	171	R	0.172	14.94	D	9.33	4.76	9.41	4.93
	NSM_d_2x1.4x10_1	R	120	8.41	19.09	17.4	540	0.253	C	2052	171	R	0.172	15.69	S	9.33	4.76	9.41	6.88
	NSM_c_3x1.4x10_1	R	120	8.41	19.09	17.4	540	0.253	C	2052	171	R	0.258	15.40	D	10.11	2.47	10.02	5.94
	NSM_d_3x1.4x10_1	R	120	8.41	19.09	17.4	540	0.253	C	2052	171	R	0.258	14.87	S	10.11	2.47	10.02	8.11
[14]	B1	T	300	5.24	10.47	48.0	400	0.064	C	2000	150	R	0.016	33.13	D	64.13	46.33	53.50	46.33
	B2	T	300	5.24	10.47	48.0	400	0.064	C	2000	150	R	0.016	33.75	D	64.13	46.33	53.50	46.33
	B3	T	300	5.24	10.47	48.0	400	0.064	C	2000	150	R	0.016	37.50	D	64.13	47.79	53.50	53.23
	B4	T	300	5.24	10.47	48.0	400	0.064	C	2000	150	R	0.016	46.25	D	64.13	47.79	53.50	53.23
	B5	T	300	5.24	10.47	48.0	400	0.064	C	2000	150	R	0.016	49.38	F	64.13	47.79	53.50	53.23
	B6	T	300	5.24	10.47	48.0	400	0.064	C	2000	150	R	0.016	46.88	F	64.13	47.79	53.50	53.23
	B7	T	300	5.24	10.47	48.0	400	0.064	C	2000	150	R	0.016	50.00	F	64.13	47.79	53.50	53.23
	B8	T	300	5.24	10.47	48.0	400	0.064	C	2000	150	R	0.016	50.00	F	64.13	47.79	53.50	53.23
[20]	BFC3	T	381	5.44	13.37	36.0	357	0.056	C	1550	165	C	0.045	186.30	D	147.47	65.76	137.35	63.78
	BFC4	T	381	5.44	13.37	36.0	357	0.056	C	1550	165	C	0.080	206.80	D	194.52	73.10	188.29	72.97
	BFG4	T	381	5.44	13.37	36.0	357	0.056	G	800	41	C	0.041	180.20	D	145.46	81.65	115.38	81.57
[21]	BR1-a	R	200	4.73	10.81	15.0	496	0.127	C	2400	129	B	0.101	74.11	D	82.27	62.91	65.56	15.59
	BR1-b	R	200	4.73	10.81	15.0	510	0.216	C	2400	129	C	0.101	109.50	C	104.39	91.83	99.36	28.06
	BR2-a	R	200	4.73	10.81	15.0	496	0.127	C	2400	129	C	0.201	85.14	D	96.78	33.61	82.76	17.49
	BR2-b	R	200	4.73	10.81	15.0	510	0.216	C	2400	129	C	0.201	118.50	C	114.87	42.42	115.65	30.14
[22]	C-A	R	200	5.49	12.09	20.0	534	0.063	C	1940	201	C	0.156	10.15	C	7.40	6.82	7.94	1.98
	C-B	R	200	5.49	12.09	33.0	534	0.038	C	1940	201	C	0.094	11.65	D	8.31	6.83	8.04	3.37
	C-C	R	200	5.49	12.09	40.0	534	0.031	C	1940	201	C	0.078	11.02	D	7.79	6.82	8.66	3.69
	C-D	R	200	5.49	12.09	63.0	534	0.020	C	1940	201	C	0.049	11.32	D	7.59	6.38	8.53	3.60
	C-E	R	200	5.49	12.09	53.0	534	0.024	C	1940	201	C	0.059	13.35	D	8.64	6.48	8.03	3.84
	C-F	R	200	5.49	12.09	20.0	534	0.126	C	1940	201	C	0.156	11.75	C	9.25	9.68	9.45	1.66
	C-G	R	200	5.49	12.09	33.0	534	0.076	C	1940	201	C	0.094	13.27	D	10.23	9.96	10.11	2.87
	C-H	R	200	5.49	12.09	63.0	534	0.040	C	1940	201	C	0.049	13.77	D	10.16	12.46	11.33	6.63
	C-I	R	200	5.49	12.09	53.0	534	0.047	C	1940	201	C	0.059	14.90	D	11.06	12.61	10.62	3.07
	C-T	R	200	5.49	12.09	20.0	534	0.063	C	1940	201	C	0.467	14.47	D	11.86	5.26	12.58	5.39
	C-U	R	200	5.49	12.09	20.0	534	0.126	C	1940	201	C	0.467	17.45	D	12.27	5.05	12.97	5.16
[23]	A1	T	300	5.24	10.47	48.0	400	0.064	C	1918	111	C	0.036	35.00	D	73.63	46.33	69.96	46.33
	A2	T	300	5.24	10.47	48.0	400	0.064	C	1918	111	C	0.036	41.88	D	73.63	59.09	69.96	28.56
	A3	T	300	5.24	10.47	48.0	400	0.064	C	1918	111	C	0.036	45.63	D	73.63	59.09	69.96	28.56
	A4	T	300	5.24	10.47	48.0	400	0.064	C	1918	111	C	0.036	49.38	D	73.63	59.09	69.96	28.56
	A5	T	300	5.24	10.47	48.0	400	0.064	C	1918	111	C	0.036	36.88	D	73.63	59.09	69.96	28.56
	A6	T	300	5.24	10.47	48.0	400	0.064	C	1918	111	C	0.036	43.75	D	73.63	59.09	69.96	28.56
	A7	T	300	5.24	10.47	48.0	400	0.064	C	1918	111	C	0.036	47.50	D	73.63	59.09	69.96	28.56
[24]	V1R1	R	100	3.42	10.27	45.3	730	0.054	C	2740	161	R	0.049	12.57	C	9.94	10.22	8.49	7.95
	V2R2	R	100	3.27	9.80	48.9	730	0.072	C	2740	161	R	0.088	19.62	D	17.34	10.34	14.06	11.68
	V3R2	R	100	3.33	10.00	42.8	730	0.090	C	2740	161	R	0.102	20.47	D	17.24	10.26	13.54	12.37
	V4R3	R	100	3.23	9.68	46.4	524	0.095	C	2740	161	R	0.137	23.72	D	21.73	9.56	18.65	19.25
[25]	B1	T	300	5.13	10.26	45.0	400	0.073	C	1408	123	C	0.028	58.63	D	74.03	61.46	72.51	29.84
	B2	T	300	5.13	10.26	45.0	400	0.073	C	1525	140	R	0.028	62.06	F	76.41	56.66	73.72	53.35
	B3	T	300	5.13	10.26	45.0	400	0.073	C	2000	150	R	0.034	68.88	F	72.24	56.34	73.24	62.24
	B4	T	300	5.13	10.26	45.0	400	0.073	G	1000	45	R	0.056	64.19	D	90.26	30.12	73.24	63.05
	B5	T	300	5.13	10.26	45.0	400	0.073	G	655	41	C	0.037	68.75	D	76.96	60.55	71.95	55.84
[26]	CRD-NSM	R	200	4.11	11.73	31.3	426	0.048	C	1878	121	C	0.064	48.63	D	42.45	31.01	40.39	15.91
	NSM-PL-25	R	200	4.11	11.73	31.3	426	0.048	C	2453	165	R	0.046	45.24	D	40.49	32.12	29.43	24.26
	NSM-PL-15	R	200	4.11	11.73	31.3	426	0.048	C	2453	165	R	0.027	43.83	F	31.16	29.20	27.72	21.90
[27]	R-1	R	150	5.00	12.38	34.3	362	0.071	A	1450	63	C	0.044	30.92	D	28.76	22.70	23.90	14.81
	R-2	R	150	5.00	12.38	34.3	362	0.071	A	1450	63	C	0.094	43.16	D	33.50	21.64	26.02	19.11
	R-3	R	150	5.00	12.38	34.3	362	0.071	A	1450	63	C	0.143	45.64	D	40.52	20.48	28.11	22.07
[28]	B500	R	150	4.69	11.72	36.5	532	0.073	C	2068	131	R	0.101	28.68	D	59.64	27.46	48.10	27.46
	B1200	R	150	4.69	11.72	36.5	532	0.073	C	2068	131	R	0.101	37.86	D	59.64	27.46	48.10	27.46
	B1800	R	150	4.69	11.72	36.5	532	0.073	C	2068	131	R	0.101	55.02	D	59.64	33.51	48.10	26.35
	B2900	R	150	4.69	11.72	36.5	532	0.073	C	2068	131	R	0.101	59.88	C	59.64	47.15	48.10	26.35
[29]	NSM-S1	R	120	2.11	6.34	52.2	788	0.029	C	2740	159	R	0.035	11.99	D	7.92	9.11	6.96	6.19
	NSM-S2	R	120	2.11	6.34	52.2	788	0.049	C	2740	159	R	0.069	14.00	D	14.16	12.07	11.50	13.78
	NSM-S3	R	120	2.11	6.34	52.2	788	0.074	C	2740	159	R	0.104	14.49	D	21.41	8.22	16.38	16.85
[30]	B.1	T	550	4.17	11.11	49.5	558	0.036	C	2068	122	R	0.017	232.00	D	158.91	69.24	131.96	73.94
	B.2	T	550	4.17	11.11	52.8	558	0.034	C	2068	122	R	0.019	240.00	D	167.56	51.06	137.21	106.79
	C.1	T	550	4.17	11.11	52.7	558	0.034	C	1970	147	C	0.015	225.00	F	171.11	105.51	136.76	49.48
	C.2	T	550	4.17	11.11	50.1	558	0.036	C	1970	147	C	0.016	237.00	F	169.17	78.43	163.78	50.64
	D.1	T	550	4.17	11.11	50.1	558	0.036	G	690	41	C	0.018	234.00	D	160.85	70.72	161.03	70.83
	D.2	T	550	4.17	11.11	35.2	558	0.051	G	690	41	C	0.025	219.00	D	166.62	52.16	148.92	52.13
[31]	A1	R	180	4.44	13.33	24.1	530	0.053	C	2922	172	R	0.112	67.20	D	64.01	29.62	51.73	38.10
	A2	R	180	4.44	13.33	20.6	530	0.062	C	2922	172	R	0.131	91.00	D	65.17	35.55	49.33	35.62

(*continued on next page*)

Table 1 (*continued*)

Name		Cross-section				Mechanical properties			NSM composite					Exp results		Analytical M_{th} [kNm]			
		S	b_w [mm]	a/d	l/d	f_{cm} [MPa]	f_{sy} [MPa]	ρ_s	F	f_{fk} [MPa]	E_f [GPa]	B	$\rho\rho_f$	M_{exp} [kNm]	FM	[2]	[16]	[17]	[1]
	B1	R	180	4.44	13.33	21.8	530	0.062	C	2922	172	R	0.131	66.99	D	62.40	33.67	47.39	34.48
	B2	R	180	4.44	13.33	22.5	530	0.060	C	2922	172	R	0.127	90.93	D	63.07	34.17	47.80	34.93
	C1	R	150	5.38	16.15	41.5	563	0.153	C	2250	163	R	0.043	86.38	C	81.91	79.69	75.56	50.07
	C2	R	150	5.32	15.97	37.7	530	0.080	C	2250	163	R	0.095	74.90	D	61.10	30.32	55.96	47.22
	C3	R	150	5.32	15.97	43.5	542	0.063	C	2250	163	R	0.124	77.84	D	76.07	22.90	62.73	53.50
[32]	B1	R	150	4.61	12.14	50.0	530	0.064	C	2580	157	R	0.062	48.17	F	40.72	37.47	30.54	32.14
	B2	R	150	4.61	12.14	50.0	530	0.064	C	2580	157	R	0.124	63.75	D	56.50	25.30	42.36	40.55
	B4	R	150	4.61	12.14	50.0	530	0.064	C	2500	153	R	0.067	49.21	D	41.06	33.48	36.77	31.40
	B5	R	150	4.61	12.14	50.0	530	0.064	C	2500	153	R	0.133	64.70	D	57.25	25.84	42.79	40.79
[33]	6-1Fa	R	152	8.46	19.04	37.2	490	0.180	C	1648	136	R	0.057	30.27	C	27.05	26.81	28.15	24.75
	6-1Fb	R	152	8.46	19.04	37.2	490	0.180	C	1648	136	R	0.057	28.32	C	27.05	26.81	28.15	24.75
	6-2Fa	R	152	8.46	19.04	37.2	490	0.180	C	1648	136	R	0.115	30.46	C	29.35	21.23	30.35	27.11
	6-2Fb	R	152	8.46	19.04	37.2	490	0.180	C	1648	136	R	0.115	32.84	C	29.35	21.23	30.35	27.11
	9-1Fa	R	229	8.37	18.83	37.2	510	0.120	C	1648	136	R	0.038	34.40	C	30.36	28.92	30.08	26.35
	9-1Fb	R	229	8.37	18.83	37.2	510	0.120	C	1648	136	R	0.038	33.38	C	30.36	28.92	30.08	26.35
	9-2Fa	R	229	8.37	18.83	37.2	510	0.120	C	1648	136	R	0.076	45.16	C	34.82	31.42	34.52	31.31
	9-2Fb	R	229	8.37	18.83	37.2	510	0.120	C	1648	136	R	0.076	43.66	C	34.82	31.42	34.52	31.31
	12-1Fa	R	305	8.37	18.83	37.2	510	0.090	C	1648	136	R	0.029	36.08	F	30.71	30.08	32.45	27.26
	12-1Fb	R	305	8.37	18.83	37.2	510	0.090	C	1648	136	R	0.029	37.80	F	30.71	30.08	32.45	27.26
	12-2Fa	R	305	8.37	18.83	37.2	510	0.090	C	1648	136	R	0.057	41.20	C	36.09	32.30	34.43	29.79
	12-2Fb	R	305	8.37	18.83	37.2	510	0.090	C	1648	136	R	0.057	50.92	C	36.09	32.30	34.43	29.79
[34]	E-6-RT-1	R	254	6.88	19.61	43.3	667	0.038	C	2776	141	R	0.079	8.50	D	8.06	8.87	5.93	6.37
	E-6-RT-2	R	254	6.88	19.61	43.3	667	0.038	C	2776	141	R	0.079	8.90	D	8.06	8.87	5.93	6.37
	E-3-RT-1	R	254	6.88	19.61	43.3	667	0.038	C	2776	141	R	0.079	8.00	D	8.22	9.15	6.03	5.28
	E-3-RT-2	R	254	6.88	19.61	43.3	667	0.038	C	2776	141	R	0.079	8.50	D	8.22	9.15	6.03	5.28
	G-6-RT-1	R	254	6.88	19.61	43.3	667	0.038	C	2776	141	R	0.079	6.30	D	8.06	8.87	5.93	6.37
	G-6-RT-2	R	254	6.88	19.61	43.3	667	0.038	C	2776	141	R	0.079	6.90	D	8.06	8.87	5.93	6.37
[35]	S-7/16″Gr-1	T	305	3.97	7.95	29.7	414	0.067	C	2068	124	R	0.061	74.25	D	67.49	47.91	57.15	41.64
	S-7/16″Gr-2	T	305	3.97	7.95	29.7	414	0.067	C	2068	124	R	0.061	72.05	D	67.49	47.91	57.15	41.64
	S-9/16″Gr-1	T	305	3.97	7.95	29.7	414	0.067	C	2068	124	R	0.061	78.65	D	67.49	47.91	57.15	41.64
	S-9/16″Gr-2	T	305	3.97	7.95	29.7	414	0.067	C	2068	124	R	0.061	75.79	D	67.49	47.91	57.15	41.64
	S-11/16″Gr-1	T	305	3.97	7.95	29.7	414	0.067	C	2068	124	R	0.061	77.77	D	67.49	47.91	57.15	41.64
	S-11/16″Gr-2	T	305	3.97	7.95	29.7	414	0.067	C	2068	124	R	0.061	70.94	D	67.49	47.91	57.15	41.64
	B-7/16″Gr-1	T	305	3.97	7.95	29.7	414	0.067	C	2068	124	C	0.060	77.55	D	68.85	48.62	58.12	22.56
	B-7/16″Gr-2	T	305	3.97	7.95	29.7	414	0.067	C	2068	124	C	0.060	81.08	D	68.85	48.62	58.12	22.56
	B-9/16″Gr-1	T	305	3.97	7.95	29.7	414	0.067	C	2068	124	C	0.060	80.19	D	68.51	48.44	57.89	22.49
	B-9/16″Gr-2	T	305	3.97	7.95	29.7	414	0.067	C	2068	124	C	0.060	75.35	D	68.51	48.44	57.89	22.49
	B-11/16″Gr-1	T	305	3.97	7.95	29.7	414	0.067	C	2068	124	C	0.060	82.40	D	68.17	48.26	57.65	22.42
	B-11/16″Gr-2	T	305	3.97	7.95	29.7	414	0.067	C	2068	124	C	0.060	77.77	D	68.17	48.26	57.65	22.42
[36]	A1	R	200	3.32	10.78	41.0	460	0.148	C	1596	124	C	0.046	90.80	D	98.43	80.20	89.07	8.69
	A2	R	200	3.32	10.78	41.0	460	0.148	C	1596	124	C	0.046	91.80	D	98.43	80.20	89.07	35.16
	A3	R	200	3.32	10.78	41.0	460	0.148	C	1596	124	C	0.046	93.60	D	98.43	83.72	89.07	35.30
	A4	R	200	3.32	10.78	41.0	460	0.148	C	1596	124	C	0.046	101.60	D	98.43	96.13	89.07	35.30
	B1	R	200	3.32	10.78	41.0	460	0.074	C	1596	124	C	0.046	50.00	D	60.49	40.11	53.15	17.26
	B2	R	200	3.32	10.78	41.0	460	0.074	C	1596	124	C	0.046	61.60	D	60.49	55.39	53.15	17.26
	C1	R	200	3.26	10.58	41.0	454	0.037	C	1596	124	C	0.046	26.88	D	44.97	17.78	35.66	17.78
	C2	R	200	3.26	10.58	41.0	454	0.037	C	1596	124	C	0.046	29.20	D	44.97	17.78	35.66	17.78
	C3	R	200	3.26	10.58	41.0	454	0.037	C	1596	124	C	0.046	37.60	D	44.97	17.78	35.66	9.39
	C4	R	200	3.26	10.58	41.0	454	0.037	C	1596	124	C	0.046	38.40	D	44.97	33.50	35.66	25.96
	C5	R	200	3.26	10.58	41.0	454	0.037	C	1596	124	C	0.046	35.20	D	45.38	17.78	35.97	17.78
	C6	R	200	3.26	10.58	41.0	454	0.037	C	1596	124	C	0.046	36.00	D	45.38	17.78	35.97	9.34
	C7	R	200	3.26	10.58	41.0	454	0.037	C	1596	124	C	0.046	40.80	D	45.38	33.92	35.97	26.23
	C8	R	200	3.26	10.58	41.0	454	0.037	C	1250	134	C	0.064	26.80	D	47.54	17.78	52.60	17.78
	C9	R	200	3.26	10.58	41.0	454	0.037	C	1250	134	C	0.064	43.60	D	47.54	39.25	52.60	32.87
	C10	R	200	3.26	10.58	41.0	454	0.037	G	756	45	C	0.039	28.40	D	36.61	17.78	32.22	17.78
	C11	R	200	3.26	10.58	41.0	454	0.037	G	756	45	C	0.039	44.80	D	36.61	25.90	32.22	20.23
[37]	S-C 6 (VC30)	R	150	3.28	11.48	37.5	600	0.086	C	1875	146	C	0.067	58.50	D	48.05	31.46	44.30	20.65
	S-C 6 (270-R)	R	150	3.28	11.48	36.5	600	0.089	C	1875	146	C	0.069	53.30	D	47.61	31.05	43.92	20.38
	S-C 6 (210-R)	R	150	3.28	11.48	36.7	600	0.088	C	1875	146	C	0.069	44.00	D	47.70	31.13	43.99	20.43
	S-C 6 (VC60)	R	150	3.28	11.48	66.5	600	0.049	C	1875	146	C	0.038	65.40	D	52.35	39.99	45.42	25.65
	S-C 6 (270-M)	R	150	3.28	11.48	38.1	600	0.085	C	1875	146	C	0.066	73.20	D	48.31	31.70	44.52	20.80
	S-C 12 (VC30)	R	150	3.28	11.48	35.1	600	0.092	C	1875	146	C	0.144	59.20	C	63.99	41.99	59.60	11.95
	S-C 12 (VC60)	R	150	3.28	11.48	67.2	600	0.048	C	1875	146	C	0.075	43.90	D	67.51	57.07	60.34	32.18
[38]	1a	R	275	1.92	6.41	41.9	481	0.055	C	1200	100	R	0.069	306.00	D	208.39	75.45	178.74	75.29
	1b	R	275	1.92	6.41	41.9	481	0.055	C	1200	100	R	0.069	299.30	D	208.39	75.45	178.74	75.29
[39]	C3	R	200	4.96	13.74	60.7	490	0.054	C	4140	230	R	0.227	160.60	D	162.13	65.14	131.96	65.33
	E3	R	200	4.96	13.74	60.7	490	0.054	C	4140	230	R	0.227	182.00	D	162.13	65.14	131.96	65.33
	E4	R	200	4.96	13.74	60.7	490	0.054	C	4140	230	R	0.227	197.60	F	162.13	65.14	131.96	65.33
[40]	B2600	R	150	4.69	11.72	31.1	576	0.093	G	760	41	C	0.039	48.90	C	40.27	36.57	33.92	16.30

Table 1 (*continued*)

Name		Cross-section				Mechanical properties			NSM composite					Exp results		Analytical M_{th} [kNm]			
		S	b_w [mm]	a/d	l/d	f_{cm} [MPa]	f_{sy} [MPa]	ρ_s	F	f_{fk} [MPa]	E_f [GPa]	B	$\rho\rho_f$	M_{exp} [kNm]	FM	[2]	[16]	[17]	[1]
	B2800	R	150	4.69	11.72	31.1	576	0.093	G	760	41	C	0.039	48.36	C	40.27	36.57	33.92	16.30
	B3200	R	150	4.69	11.72	31.1	576	0.093	G	760	41	C	0.039	49.14	C	40.27	36.57	33.92	16.30
[41]	A9	R	100	5.87	13.33	27.9	452	0.141	C	1020	109	C	0.204	20.20	D	17.93	10.24	18.84	10.19
	A10	R	100	5.87	13.33	27.9	452	0.141	C	1020	109	C	0.204	19.67	D	17.93	10.24	18.84	10.19
	B8	R	100	5.20	12.00	27.9	441	0.199	C	1020	109	C	0.204	23.56	C	19.63	9.77	20.36	9.69
[42]	VL1	R	200	2.51	6.85	31.1	552	0.066	C	2783	157	R	0.100	33.44	S	63.54	24.21	47.61	32.28
	VL2	R	200	2.60	6.57	31.1	548	0.065	C	2783	157	R	0.078	62.19	S	80.92	30.80	59.04	45.17
	VL3	R	200	2.58	6.30	31.1	588	0.069	C	2783	157	R	0.066	78.71	S	96.07	51.20	73.21	51.43
[43]	B3	R	150	3.28	10.93	60.0	510	0.045	C	1970	136	C	0.056	48.40	D	38.18	37.23	29.38	12.02
	B4	R	150	3.28	10.93	60.0	510	0.045	C	2166	130	C	0.069	44.34	D	42.08	38.71	29.86	12.32
[44]	RW1F	R	150	5.92	13.16	36.6	408	0.058	G	743	40	C	0.053	21.84	F	15.05	12.35	11.98	8.78
	RW2F	R	150	5.92	13.16	36.6	408	0.029	G	743	40	C	0.106	23.03	F	17.59	8.13	11.85	8.29
[45]	LB1C1	R	160	3.28	9.84	32.4	545	0.085	C	2350	170	C	0.081	43.64	D	49.87	39.37	43.02	12.00
	LB2C1	R	160	3.28	9.84	32.4	545	0.085	C	2350	170	C	0.163	46.88	D	65.55	28.15	56.20	18.60
	LA2C1	R	160	3.28	9.84	32.4	545	0.085	C	2350	170	C	0.163	45.80	D	65.55	28.15	56.20	18.60
	LB1G1	R	160	3.28	9.84	32.4	545	0.085	G	1350	64	C	0.047	39.68	F	40.63	30.12	32.53	18.96
	LB2G1	R	160	3.28	9.84	32.4	545	0.085	G	1350	64	C	0.094	44.88	D	48.59	32.50	41.07	21.15
	LA2G1	R	160	3.28	9.84	32.4	545	0.085	G	1350	64	C	0.094	44.24	D	48.59	32.50	41.07	21.15
	LB1G2	R	160	3.28	9.84	32.4	545	0.085	G	1350	64	C	0.105	42.32	D	50.08	36.10	41.32	21.88

Note: S = shape: R = rectangular cross-section; T = T cross-section. b_w = width of the beam web. l = distance between supports. F = fiber: C = carbon; G = glass. B = bars: R = rectangular bar; C = circular bar. Failure mode (FM): D = debonding; C = concrete crushing; F = failure of NSM composite; S = beam shear failure.

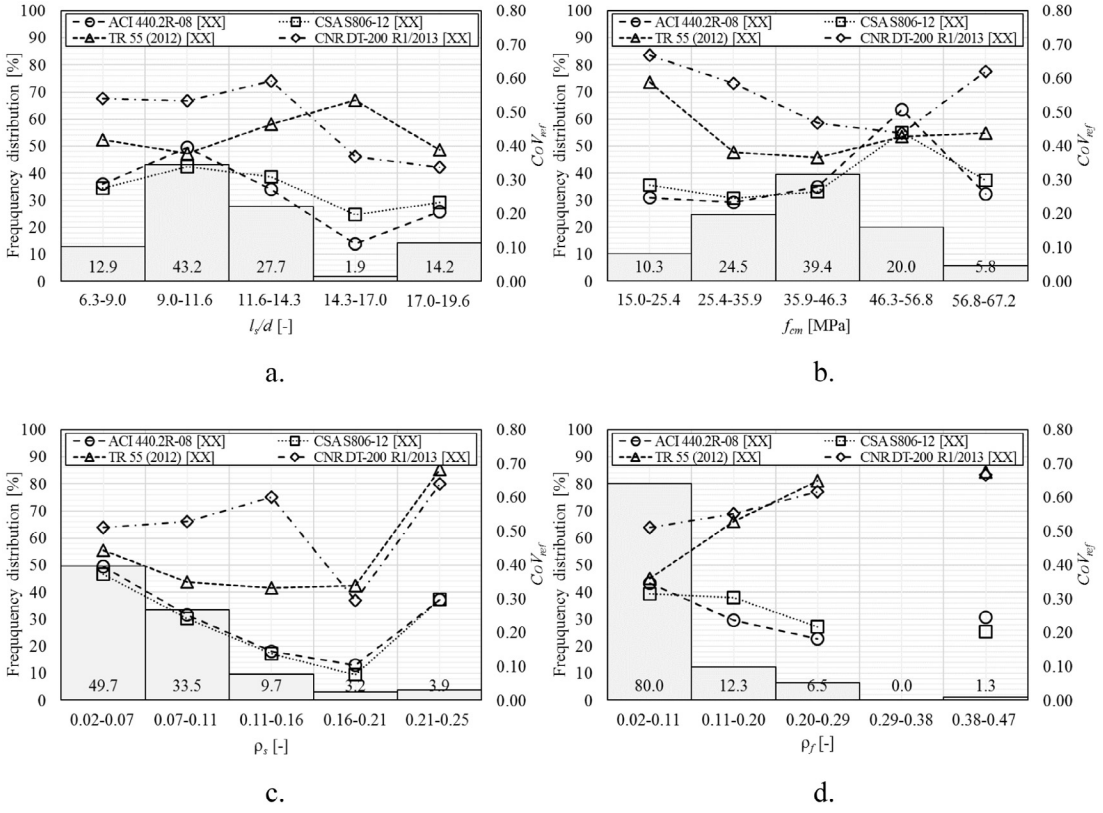

Fig. 1. Frequency distribution of specimens in the database and, on secondary axes, CoV_{ref} for each analytical model considered for different data ranges of a) l_s/d, b) f_{cm}, c) ρ_s, and d) ρ_f.

where A_s and A_c are the cross-sectional areas of tensile steel and concrete, respectively, and f_y is the (average) steel yielding stress. ρ_s varies between 0.02 and 0.25, with 83.2% of the specimens having ρ_s lower than 0.11. The NSM reinforcement mechanical ratio ρ_f (Fig. 1d) is:

$$\rho_f = \frac{A_f E_f \varepsilon^*_{fu}}{A_c f_{cm}} \tag{18}$$

ρ_f varies between 0.02 and 0.47, with 80% of the specimens having ρ_f lower than 0.11.

Specimens in the database failed due to different failure modes (FM). 112 beams (72%) failed due to debonding of the FRP reinforcement (indicated with "D" in Table 1), whereas the remaining failed due to rupture of the FRP reinforcement (16 beams, 10% – indicated with "F" in Table 1), concrete crushing (22 beams, 14% – indicated with "C" in Table 1), or shear deficiency (5 beams, 3% – indicated with "S" in Table 1).

4. Assessment of the analytical models considered

The accuracy of each analytical model considered was evaluated by comparing the maximum bending moment measured experimentally, M_{exp}, with the corresponding maximum bending moment obtained with the analytical procedure, M_{th}. The analytical maximum bending moment was obtained by enforcing the equilibrium of the beam cross-section assuming elasto-plastic behavior of concrete and steel and linear-elastic behavior up to ε_{fd} of NSM reinforcement. Following the indications of each guideline considered, different concrete stress-strain analytical models were employed. The elasto-plastic model proposed by Hognestad [46] was used to model the concrete stress-strain behavior when assessing the American and Canadian guidelines, whereas the parabola-rectangle model proposed by EN 1992-1-1 [47] was employed when assessing the English and extended Italian guidelines. The reinforcing steel was assumed elasto-perfectly plastic, whereas the NSM reinforcement was described by a linear-elastic behavior up to ε_{fd}. It should be noted that mean values of all parameters were employed and all safety factors and partial coefficients provided by the models were assumed equal to 1.0. Furthermore, when values of the adhesive tensile strength f_{at} were not specified by the authors of the tests, Eq. (8) was assumed to be verified when assessing the TR 55 [16] model. Values of M_{th} obtained from the analytical models considered are reported in Table 1 for each specimen included in the database.

The accuracy of each analytical model was assessed by computing the average $\bar{r}$ and coefficient of variation CoV of the ratios r between the ith analytical and experimental maximum bending moments:

$$r_i = \frac{M_{th,i}}{M_{exp,i}} \tag{19}$$

$$\bar{r} = \frac{\sum_{i=1}^{N} M_{th,i}/M_{exp,i}}{N} \tag{20}$$

$$CoV = \sqrt{\frac{\sum_{i=1}^{N}(r_i - \bar{r})^2}{\bar{r}^2(N-1)}} \tag{21}$$

where N is the number of specimens in the database, equal to 155 in this study. In addition, the discrepancy between analytical and experimental results was measured by computing a reference coefficient of variation CoV_{ref} with respect to the perfect match average ratio $\bar{r}_{ref}$=1.0:

$$CoV_{ref} = \sqrt{\frac{\sum_{i=1}^{N}(r_i - \bar{r}_{ref})^2}{N-1}} \tag{22}$$

5. Results and discussion

Values of $\bar{r}$, CoV, and CoV_{ref} with respect to all data included in the database are reported in Table 2 for each analytical model considered. Comparisons between analytical and experimental maximum bending moment for the 155 beams included in the database are shown in Fig. 2 (left-hand side). Call-outs for a limited

Table 2
Results of the assessment of the analytical models considered.

	ACI 440.R2-08 [2]			CSA S806-12 [17]			TR 55 [16]			CNR-DT 200 R1/2013 [1]		
All data	$\bar{r}$	CoV [%]	CoV_{ref}[%]	$\bar{r}$	CoV [%]	CoV_{ref}[%]	$\bar{r}$	CoV [%]	CoV_{ref}[%]	$\bar{r}$	CoV [%]	CoV_{ref}[%]
–	1.02	32.51	32.60	0.90	29.10	30.84	0.70	28.86	41.58	0.55	27.10	52.82
All data $\varepsilon_{fd} = \varepsilon^{*}_{fu}$	$\bar{r}$	CoV [%]	CoV_{ref} [%]	$\bar{r}$	CoV [%]	CoV_{ref}[%]	$\bar{r}$	CoV [%]	CoV_{ref}[%]	$\bar{r}$	CoV [%]	CoV_{ref}[%]
–	1.13	38.06	40.12	1.16	37.85	40.94	1.17	37.34	41.06	1.17	37.34	41.06
l_s/d [–]	$\bar{r}$	CoV [%]	CoV_{ref}[%]	$\bar{r}$	CoV [%]	CoV_{ref}[%]	$\bar{r}$	CoV [%]	CoV_{ref}[%]	$\bar{r}$	CoV [%]	CoV_{ref}[%]
6.3–9.0	0.98	30.14	28.82	0.80	24.29	27.55	0.60	23.61	41.97	0.53	51.00	54.02
9.0–11.6	1.19	29.29	39.65	1.05	32.15	33.95	0.80	40.40	37.89	0.58	56.76	53.40
11.6–14.3	0.87	27.82	27.23	0.76	25.94	30.86	0.57	31.42	46.50	0.43	36.25	59.27
14.3–17.0	0.91	9.43	11.13	0.81	7.89	19.77	0.54	62.06	53.49	0.63	8.52	37.02
17.0–19.6	0.87	19.06	20.71	0.80	15.53	23.31	0.78	42.19	38.87	0.71	24.13	33.76
f_{cm} [MPa]	$\bar{r}$	CoV [%]	CoV_{ref}[%]	$\bar{r}$	CoV [%]	CoV_{ref}[%]	$\bar{r}$	CoV [%]	CoV_{ref}[%]	$\bar{r}$	CoV [%]	CoV_{ref}[%]
15.0–25.4	0.82	20.97	24.75	0.75	19.11	28.40	0.45	49.66	58.89	0.34	37.90	66.89
25.4–35.9	0.97	24.08	23.26	0.83	21.38	24.58	0.64	19.18	38.14	0.44	36.09	58.50
35.9–46.3	1.03	27.18	27.98	0.91	27.58	26.44	0.73	33.90	36.59	0.59	37.69	46.78
46.3–56.8	1.22	38.31	50.66	1.06	41.66	43.96	0.86	47.69	42.73	0.76	49.18	43.91
56.8–67.2	0.91	28.16	25.77	0.79	28.89	29.90	0.68	46.55	43.78	0.39	36.83	62.12
ρ_s [–]	$\bar{r}$	CoV [%]	CoV_{ref}[%]	$\bar{r}$	CoV [%]	CoV_{ref}[%]	$\bar{r}$	CoV [%]	CoV_{ref}[%]	$\bar{r}$	CoV [%]	CoV_{ref}[%]
0.02–0.07	1.08	36.35	39.68	0.93	39.80	37.35	0.74	48.89	44.46	0.59	52.00	51.12
0.07–0.11	1.01	25.18	25.34	0.88	24.01	24.25	0.68	21.25	35.03	0.52	42.10	52.85
0.11–0.16	0.93	14.43	14.57	0.89	8.88	13.75	0.74	28.38	33.29	0.44	52.44	60.15
0.16–0.21	0.91	5.86	10.37	0.94	5.87	7.63	0.72	29.37	33.92	0.76	26.10	29.60
0.21–0.25	0.75	22.64	29.68	0.74	21.63	29.86	0.36	69.83	68.18	0.37	30.62	64.00
ρ_f [–]	$\bar{r}$	CoV [%]	CoV_{ref}[%]	$\bar{r}$	CoV [%]	CoV_{ref}[%]	$\bar{r}$	CoV [%]	CoV_{ref}[%]	$\bar{r}$	CoV [%]	CoV_{ref}[%]
0.02–0.11	1.06	32.31	34.60	0.92	33.27	31.55	0.77	36.14	36.13	0.57	49.45	51.17
0.11–0.20	0.90	24.60	23.74	0.78	27.16	30.32	0.49	32.35	52.92	0.49	44.08	55.24
0.20–0.29	0.88	16.41	18.23	0.82	16.34	21.74	0.36	33.51	64.88	0.39	28.37	61.69
0.29–0.38	–	–	–	–	–	–	–	–	–	–	–	–
0.38–0.47	0.76	10.86	24.56	0.81	11.04	20.35	0.33	16.04	67.45	0.33	16.26	66.67

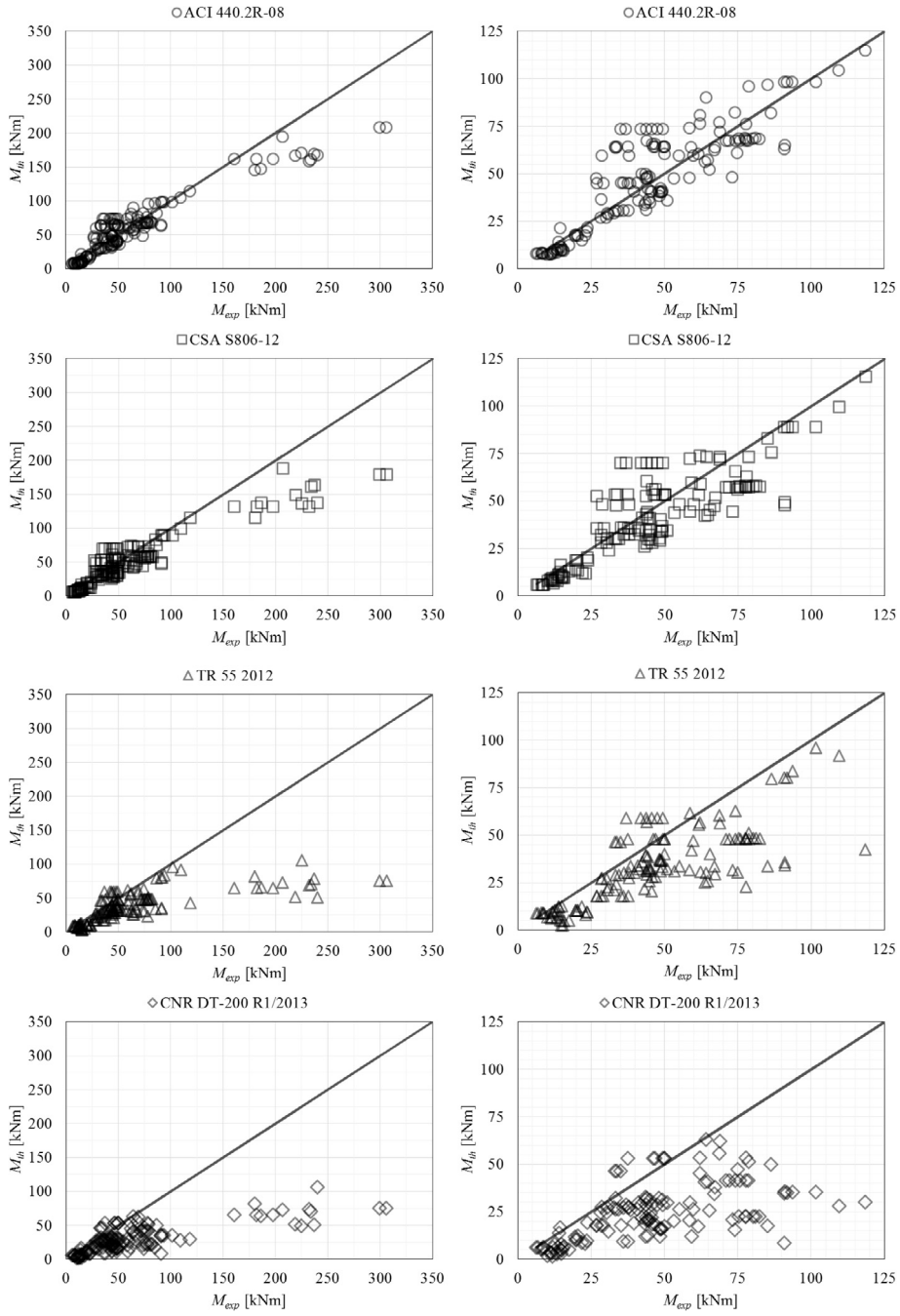

Fig. 2. Comparison between analytical and experimental maximum bending moment values of the 155 beams included in the database (left-hand side) and call-outs for data up to $M_{th} = M_{exp} = 125$ kNm (right-hand side).

range of data (up to $M_{th} = M_{exp} = 125$ kNm) are shown in Fig. 2 (right-hand side). Values below the line $M_{th}/M_{exp} = 1.0$ are conservative since the estimated bending moment is lower than the corresponding experimentally measured value, whereas values above the line $M_{th}/M_{exp} = 1.0$ overestimate the experimental results and, thus, are non-conservative.

The results obtained with respect to all data included in the database show that the Canadian CSA S806-12 [17] model provided the most accurate results, having a reference coefficient of variation of $CoV_{ref} = 30.84\%$. The Canadian model tended to slightly underestimate the experimental results ($\bar{r} = 0.90$), with a dispersion around the mean value of approximately 29%. Although a specific formulation to prevent NSM reinforcement debonding failure is not provided, the Canadian design approach seems particularly attractive because provides accurate results with a simple procedure. It should be noted that the CSA S806-12 [17] model does not provide a specific formulation to compute the development length of the NSM reinforcement. This approach could be misleading because it provides the full contribution (up to $\varepsilon_{fd} = 0.007$) of the NSM reinforcement regardless of the bonded length.

The accuracy of the American ACI 440.2R-08 [2] model ($CoV_{ref} = 32.60\%$) is close to that obtained with the Canadian model. Although the average of ratios between theoretical and experimental maximum bending moment values $\bar{r} = 1.02$ is approximately equal to the perfect match ratio $\bar{r}_{ref} = 1.0$, the dispersion of the results ($CoV = 32.51\%$) is higher than that obtained with the Canadian model. Similarly to the Canadian model, the ACI 440.2R-08 [2]

model provided accurate results with a simple procedure, which appears more reliable than the Canadian approach because the maximum strain in the composite is related to the NSM reinforcement failure strain through Eq. (2) and it is not a constant value. Although a formulation for computing the development length of NSM reinforcement is provided in ACI 440.2R-08 [2] (Eqs. (3) and (4)), the possibility of failure along the development length is not taken into account.

The English TR 55 [16] approach, which was developed specifically for NSM reinforcement and imposes several different analyses, tended to underestimate the experimental results ($\bar{r} = 0.70$), with a dispersion of approximately 29%. The reference coefficient of variation obtained (CoV_{ref} = 41.58%) is higher than those obtained with the Canadian and American models, which indicates a lower accuracy of TR 55 [16] with respect to CSA S806-12 [17] and ACI 440.2R-08 [2]. It should be noted that performing the analyses of the shear stresses at the adhesive-concrete and adhesive-NSM reinforcement interfaces, which in this study were assumed to be lower than the corresponding maximum values allowed, might lead to lower estimation of the maximum bending moment, which in turn would imply a lower accuracy of the model.

The less accurate estimations (CoV_{ref} = 52.82%) were obtained by extending the Italian CNR-DT 200 R1/2013 [1] EB reinforcement model to the case of NSM reinforcement. The extended Italian model tended to a large underestimation of the results ($\bar{r} = 0.55$), with a dispersion of approximately 27%. The poor accuracy obtained with the extended Italian procedure is caused by the estimated premature debonding failure of the NSM composite. The Italian procedure was calibrated for EB FRP reinforcement, which is more sensitive to debonding than NSM reinforcement [2,8,9]. Therefore, when extended to NSM strengthened beams, the Italian procedure leads to an underestimation of the maximum bending moment, provided that the same coefficient calibrated for EB reinforcement are employed. By properly revising the model proposed by CNR-DT 200 R1/2013 [1] with a new calibration of the coefficients, a higher accuracy for the case of NSM reinforcement could be obtained.

The influence of debonding failure modes on the model accuracy was evaluated by enforcing the cross-section equilibrium of the strengthened beams assuming $\varepsilon_{fd} = \varepsilon^*_{fu}$ (Table 2). When debonding is prevented (i.e. $\varepsilon_{fd} = \varepsilon^*_{fu}$), $\bar{r}$, *CoV*, and CoV_{ref} obtained with the American and Canadian guidelines increased with respect to those obtained considering the limitations imposed on the NSM reinforcement strain (see Eqs. (1) and (2) and Section 2.3). The results obtained with the English guideline assuming $\varepsilon_{fd} = \varepsilon^*_{fu}$ were similar to those obtained following the procedure proposed by TR 55 [16], with a slight increase of accuracy when $\varepsilon_{fd} = \varepsilon^*_{fu}$. The accuracy of the extended Italian guideline is the same obtained with the English guideline when $\varepsilon_{fd} = \varepsilon^*_{fu}$ is assumed, being both models based on EN 1992-1-1 [47]. These results confirm that ACI 440.2R-08 [2] and CSA S806-12 [17] can accurately predict the debonding failure, whereas the extended CNR-DT 200 R1/2013 [1] model tend to underestimate the NSM reinforcement bond capacity.

5.1. Effect of the data range on model accuracy

The accuracy of each model considered was assessed with respect to various data ranges to investigate the influence of different parameters on the analytical maximum bending moment values obtained. Data in the database were sorted in five data ranges with different l_s/d, f_{cm}, ρ_s, and ρ_f, as indicated in Fig. 1 and Table 2. $\bar{r}$, *CoV*, and CoV_{ref} (Eqs. (20)–(22)) were computed for each range and model considered and are reported in Table 2.

The results obtained showed that all analytical models except the extended Italian model have a similar accuracy (CoV_{ref} between 30% and 40%, see Table 2) for l_s/d included between 9.0 and 11.6. The English model loses its accuracy with increasing l_s/d (Fig. 1a), which might indicate that this model was calibrated using experimental results from beams with $l_s/d < 11.6$, as typically occurs with laboratory beam specimens.

The accuracy of the Canadian and American models does not appear to be affected by varying the concrete compressive strength f_{cm} up to 46.3 MPa, whereas poorly accurate results are obtained for 46.3 MPa < $f_{cm} \leqslant$ 56.8 MPa. It should be noted that, although similar CoV_{ref} values were obtained for all model for 46.3 MPa < $f_{cm} \leqslant$ 56.8 MPa (Fig. 1b), the Canadian and American approaches tend to overestimate the maximum bending moment whereas the English and extended Italian approached tend to underestimate it (see Table 1). However, values of f_{cm} higher than 35.9 MPa are not likely to be found in real reinforced concrete elements in need of strengthening. Therefore, the poor accuracy obtained for f_{cm} should not affect real NSM strengthening applications.

The influence of different ρ_s and ρ_f values could not be clearly investigated. Values of $\bar{r}$, *CoV*, and CoV_{ref} obtained should not be considered reliable statistical parameters due to the significantly different number of specimens included in each range of ρ_s and ρ_f (Fig. 1c and d, respectively).

5.2. Effect of the NSM reinforcement bonded length

The full contribution of a reinforcing material can be exploited only if the bonded length l is higher than the corresponding development length l_{db}. When the bonded length is shorter than the corresponding development length the reinforcement can provide only a fraction of the full theoretical contribution. The English TR 55 [16] and Italian CNR-DT 200 R1/2013 [1] models provide specific formulations to compute the development length and enforce a reduction of the strain attainable in the composite when $l < l_{db}$ (see Eqs. (6) and (7) and (15) and (16)). Debonding occurs when the strain in the FRP reinforcement in the cross-section where the FRP is needed, i.e. where the steel reinforcement begins to yield, is higher than the maximum strain attainable in the FRP composite, which depends on the bonded length l.

NSM reinforcements with different bonded lengths, evaluated as the distance between the composite end and the cross-section where the steel reinforcement begins to yield, are included in the database. The accuracy of the English and extended Italian procedures was assessed for different bonded length ranges. Specimens for which the steel reinforcement begins to yield outside the NSM bonded length are indicated with $l < 0$ (in this case the NSM could not provide any contribution and the beam behaves as unreinforced). When the steel reinforcement begins to yield along the NSM development length ($0 < l < l_{db}$), the composite reinforcement could not provide its full theoretical contribution. Otherwise, if the NSM bonded length is higher than the corresponding development length but shorter than the beam span ($l_{db} < l < l_s$), the composite reinforcement provides its full theoretical contribution, though debonding failure could still occur. For some specimens included in the database the NSM bonded length was higher than the corresponding beam spam ($l > l_s$). In this case the NSM reinforcement results anchored and debonding at the ends is prevented. It should be noted that anchoring the NSM reinforcement in correspondence with the supports could not be easily performed in real applications due to the presence of columns and/or walls. All specimens for which the distance between the NSM reinforcement end and the closest support was not clearly reported by the authors of the tests were included in the range $l > l_s$.

Fig. 3 shows comparisons between analytical and experimental maximum bending moment values obtained by TR 55 [16] and CNR-DT 200 R1/2013 [1] for the different bonded length

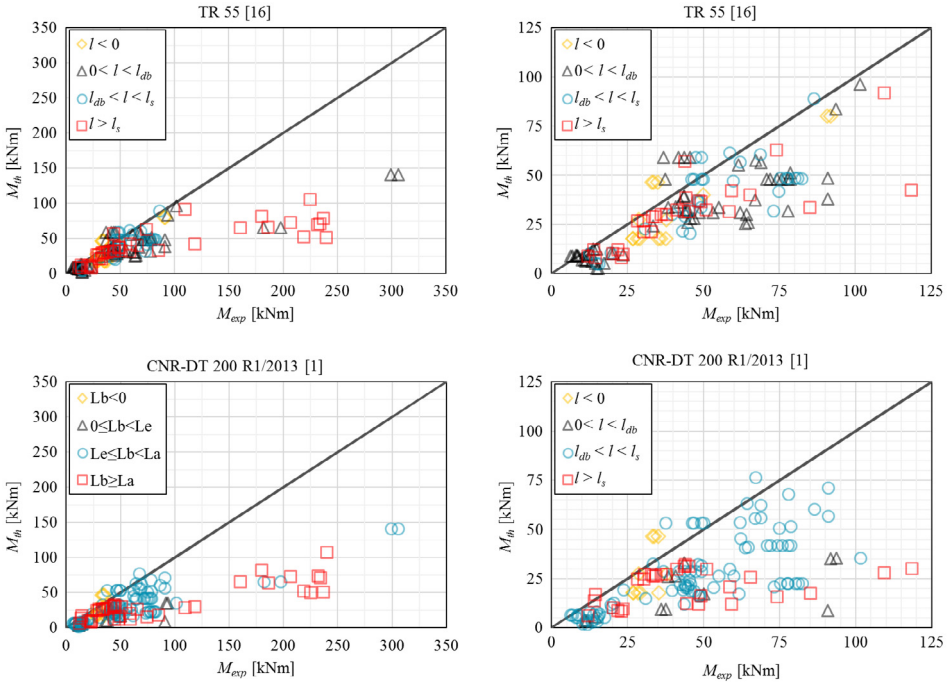

Fig. 3. Comparison between analytical and experimental maximum bending moment values of the 155 beams included in the database (left-hand side) and call-outs for data up to $M_{th} = M_{exp} = 125$ kNm (right-hand side) for different bonded length ranges.

Table 3
Results of the assessment of the English and extended Italian models for different bonded length ranges.

Model	Range of l	n (%)	$\bar{r}$	CoV [%]	CoV_{ref} [%]
TR 55 [16]	$l < 0$	15 (9.7%)	0.83	38.16	36.33
	$0 < l < l_{db}$	66 (42.9%)	0.72	42.95	41.81
	$l_{db} < l < l_s$	33 (21.4%)	0.74	31.56	35.13
	$l > l_s$	40 (26.0%)	0.62	38.86	45.44
CNR-DT 200 R1/2013 [1]	$l < 0$	10 (6.5%)	0.88	39.74	37.20
	$0 < l < l_{db}$	12 (7.8%)	0.40	48.85	65.79
	$l_{db} < l < l_s$	92 (59.7%)	0.57	44.43	50.46
	$l > l_s$	40 (26.0%)	0.51	50.87	56.24

ranges considered, whereas Table 3 reports values of $\bar{r}$, CoV, and CoV_{ref} (Eqs. (20)–(22)) obtained for each range. The number of specimens n in each range and the corresponding percentage with respect to N are also reported in Table 3. The results obtained shows that, when $l < 0$, the analytical maximum bending moment values obtained with both TR 55 [16] and CNR-DT 200 R1/2013 [1] are close to the corresponding experimental values. For $0 < l < l_{db}$ the English procedure tends to slightly underestimate the experimental values, whereas the extended Italian procedure provides highly underestimated provisions. For $l_{db} < l < l_s$ and $l > l_s$ both the English and extended Italian approaches tend to underestimate the maximum bending moment. It should be noted that results obtained with TR 55 [16] procedure for $l_{db} < l < l_s$, although slightly underestimated, are (relatively) accurate ($CoV_{ref} = 35.13\%$), which indicates that this model is able to provide accurate results when the NSM bonded length is higher than the corresponding development length, whereas its accuracy is poor for the remaining cases.

6. Conclusions

This paper presents the assessment of four analytical models for the estimation of the bending capacity of RC beams strengthened with NSM reinforcement. The NSM reinforcement design formulations proposed by the American ACI 440.2R-08 [2], English TR 55 [16], and Canadian CSA S806-12 [17] guidelines were considered. Furthermore, the procedure for EB reinforcement proposed by the Italian CNR-DT 200 R1/2013 [1] was extended to the case of NSM reinforcement. An experimental database comprised of 155 RC beams tested in flexure by 28 working groups was collected from the literature. The accuracy of each analytical model was assessed by comparing values of the maximum bending moment obtained from the analytical formulations with corresponding values measured experimentally. The results obtained with respect to all data in the database showed that the Canadian and American approaches provided the most accurate results. The Canadian model tended to slightly underestimate the experimental results, whereas the American model provided results (on average) very close to the experimental measures. These two approaches seem particularly attractive because they provide accurate results with a simple procedure. The American approach appears more reliable than the Canadian approach because the maximum strain in the composite is related to the NSM reinforcement failure strain and it is not a constant value. However, although the American approach provides a specific formulation for computing the NSM reinforcement development length, both the Canadian and American procedures do not take into account the possibility of failure along the development length.

The English procedure, which was developed specifically for NSM reinforcement, generally underestimated the experimental results providing a limited accuracy. However, it provided accurate results when the NSM bonded length was higher than the corresponding development length. The extended Italian approach generally provided underestimated results, which are attributed to the fact that the procedure adopted was originally developed for EB reinforcement that usually fails due to debonding at strain values lower than those observed for NSM reinforcement. A proper revision of the Italian EBR approach with a new coefficients calibration could highly improve the accuracy obtained for the case of NSM reinforcement.

The effect of debonding failures on the model accuracy was investigated by assuming that NSM debonding was prevented (i.e. $\varepsilon_{fd} = \varepsilon^*_{fu}$). The results obtained confirmed that the American and Canadian models can accurately predict the debonding failure, whereas the extended Italian model tend to underestimate the NSM reinforcement bond capacity.

By sorting the data included in the database in different ranges, the influence of l_s/d and f_{cm} was investigated. The results obtained indicated that the English model loses its accuracy with increasing l_s/d, which might be due to a model calibration with respect to experimental results from beams with $l_s/d < 11.6$, as typically occurs with laboratory beam specimens. The Canadian and American models were poorly accurate for concrete compressive strength values between 46.3 MPa and 56.8. However, values of f_{cm} in this range appear too high to be representative of real reinforced concrete elements in need of strengthening.

The results obtained show that, although conservative, the analytical models considered are (relatively) poorly accurate. Further studies seem to be necessary to provide reliable and accurate procedures for designing flexural strengthening with NSM reinforcement.

References

[1] CNR-DT 200 R1/2013, Guide for the design and construction of externally bonded FRP systems for strengthening existing structures, Rome, Italy: National Research Council; 2013.

[2] ACI 440.2R-08, Guide for the design and construction of externally bonded FRP systems for strengthening concrete structures, Farmington Hills, MI, USA: American Concrete Institute; 2008.

[3] L'Hermite R, Bresson J. Béton armé d'armatures collées. In RILEM Int Symp Synth Resins in Build Constr, Paris, 4–6 September 1967.

[4] Fleming CJ, King GEM. The development of structural adhesives for three original uses in South Africa. Mater Struct 1967;37:241–51.

[5] Lerchenthal CH. Bonded steel reinforcement for concrete slabs. Mater Struct 1967;37:263–9.

[6] Asplund SO. Strengthening bridge slabs with grouted reinforcement. J American Concr Inst 1949;20(6):397–406.

[7] fib, Externally bonded FRP reinforcement for RC structures - fib Bulletin 14, Lausanne, Switzerland: International Federation for Structural Concrete (fib); 2001.

[8] El-Hacha R, Rizkalla SH. Near-surface-mounted fiber-reinforced polymer reinforcements for flexural strengthening of concrete structures. ACI Struct J 2004;101(5):717–26.

[9] Bilotta A, Ceroni F, Nigro E, Pecce M. Efficiency of CFRP NSM strips and EBR plates for flexural strengthening of RC beams and loading pattern influence. Compos Struct 2015;124:163–75.

[10] De Lorenzis L, Teng JG. Near-surface mounted FRP reinforcement: An emerging technique for strengthening structures. Compos Part B: Eng 2007;38:119–43.

[11] Ceroni F, Pecce M, Bilotta A, Nigro E. Bond behavior of FRP NSM systems in concrete elements. Compos Part B: Eng 2012;43:99–109.

[12] Sharaky I, Torres L, Baena M, Miàs C. An experimental study of different factors affecting the bond of NSM FRP bars in concrete. Compos Struct 2013;99:350–65.

[13] De Lorenzis L, Nanni A. Bond between near-surface mounted FRP rods and concrete in structural strengthening. ACI Struct J 2002;99(2):123–32.

[14] Hassan T, Rizkalla S. Investigation of bond in concrete structures strengthened with near surface mounted carbon fiber reinforced polymer strips. J Compos Constr 2003;7(3):248–57.

[15] Khshain NT, Al-Mahaidi R, Abdouka K. Bond behaviour between NSM CFRP strips and concrete substrate using single-lap shear testing with epoxy adhesive. Compos Struct 2015;132:205–14.

[16] Technical Report 55, Design guidance for strengthening concrete structures using fibre composite materials. 3rd edition, Crowthorne, UK: The Concrete Society; 2012.

[17] CSA S806-12, Design and construction of building structures with fibre-reinforced polymers. Toronto, Canada: Canadian Standards Association; 2012.

[18] D'Antino T, Pellegrino C. Bond between FRP composites and concrete: assessment of design procedures and analytical models. Compos Part B: Eng 2014;60:440–56.

[19] D'Antino T, Triantafillou TC. Accuracy of design-oriented formulations for evaluating the flexural and shear capacities of FRP-strengthened RC beams. Struct Concr 2015. http://dx.doi.org/10.1002/suco.201500066.

[20] De Lorenzis L, Nanni A, La Tegola A. Flexural and shear strengthening of reinforced concrete structures with near surface mounted FRP rods. Proc. of 3rd Int. Conf. on Advanced Composite Materials in Bridges and Structures, Ottawa, Canada. p. 521–8.

[21] De Lorenzis L, Micelli F, La Tegola A. Passive and active near-surface mounted FRP rods for flexural strengthening of RC beams. Proc. of the 3rd Int. Conf. on Composites in Infrastructure (ICCI 2002).

[22] Arduini M, Nanni A, Romagnolo M, Camomilla G. Influence of concrete tensile softening on the performance of FRP strengthened RC beams: experiments. 4th Int. Conf. on Advanced Composite Materials in Bridges and Structures, Calgary, Alberta.

[23] Hassan TK, Rizkalla SH. Bond mechanism of NSM FRP bars for flexural strengthening of concrete structures. ACI Struct J 2004;101(6):830–9.

[24] Barros JAO, Fortes AS. Flexural strengthening of concrete beams with CFRP laminates bonded into slits. Cem and Concr Compos 2005;27(4):471–80.

[25] El-Hacha R, Rizkalla SH, Kotynia R. Modelling of reinforced concrete flexural members strengthened with near-surface mounted FRP reinforcement. Proc. of the 7th Int. Symp on Fiber Reinforced Polymer Reinforcement for Concrete Structures (FRPRCS-7), New Orleans. p. 1681–700.

[26] Jung WT, Park YH, Park JS, Kang JY, You YJ. Experimental investigation on flexural behavior of RC beams strengthened by NSM CFRP reinforcements. Proc. of the 7th Int. Symp on Fiber Reinforced Polymer Reinforcement for Concrete Structures (FRPRCS-7), New Orleans. p. 795–806.

[27] Kishi N, Mikami H, Kurihashi Y, Sawada S. Flexural behaviour of RC beams reinforced with NSM AFRP rods. Proc. of the Int. Symp on Bond Behaviour of FRP in Structures (BBFS 2005). p. 337–42.

[28] Teng JG, De Lorenzis L, Wang B, Li R, Wong TN, Lam L. Debonding failures of RC beams strengthened with near surface mounted CFRP strips. J Compos Constr 2006;10(2):92–105.

[29] Barros JAO, Dias SJE, Lima JLT. Efficacy of CFRP-based techniques for the flexural and shear strengthening of concrete beams. Cem Concr Compos 2007;29(3):203–17.

[30] Castro EK, Melo GS. Flexural strengthening of RC T beams with near surface mounted (NSM) FRP reinforcements. Proc. of the 8th Int. Symp on Fiber Reinforced Polymer Reinforcement for Concrete Structures (FRPRCS-8), Patras, Greece.

[31] Kotynia R. Analysis of the flexural response of NSM FRP-strengthened concrete beams. Proc. of the 8th Int. Symp on Fiber Reinforced Polymer Reinforcement for Concrete Structures (FRPRCS-8), Patras, Greece.

[32] Thorenfeldt E. Bond capacity of CFRP strips glued to concrete in sawn slits. Proc. of the 8th Int. Symp on Fiber Reinforced Polymer Reinforcement for Concrete Structures (FRPRCS-8), Patras, Greece.

[33] Yost R, Gross SP, Dinehart DW, Mildenberg JJ. Flexural behavior of concrete beams strengthened with near-surface-mounted CFRP strips. ACI Struct J 2007;104(4):430–7.

[34] Burke PJ. Low and high temperature performance of near surface mounted FRP strengthened concrete slabs. Kingston, Ontario, Canada: Queen's University; 2008.

[35] Kalayci AS. Development of surface flaw thresholds for pre-cured fiber reinforced polymer and groove size tolerance for near surface mounted fiber reinforced polymer retrofit systems. Florida International University; 2008.

[36] Soliman SM. Flexural behaviour of reinforced concrete beams strengthened with near surface mounted FRP bars. University of Sherbrooke; 2008.

[37] Al-Mahmoud F, Castel A, François R, Tourneur C. Strengthening of RC members with near-surface mounted CFRP rods. Compos Struct 2009;91:138–47.

[38] Petrina DA. Strengthening of reinforced concrete beams using anchored near surface mounted bars. McMaster University; 2009.

[39] Täljsten B, Carolin A, Nordin H. Concrete structures strengthened with near surface mounted reinforcement of CFRP. Adv in Struct Eng 2009;6(3):201–13.

[40] Wang B, Teng JG, De Lorenzis L, Zhou LM, Ou J, Jin W, et al. Strain monitoring of RC members strengthened with smart NSM FRP bars. Constr Build Mater 2009;23(4):1698–711.

[41] Ceroni F. Experimental performances of RC beams strengthened with FRP materials. Constr Build Mater 2010;24(9):1547–59.

[42] Barros JAO, Costa IG, Ventura-Gouveia A. CFRP flexural and shear strengthening technique for RC beams: Experimental and numerical research. Adv in Struct Eng 2011;14(3):551–71.

[43] Wahab N, Soudki KA, Topper T. Mechanism of bond behavior of concrete beams strengthened with near-surface-mounted CFRP rods. J Compos Constr 2011;15(1):85–92.

[44] Almusallam TH, Elsanadedy HM, Al-Salloum YA, Alsayed SH. Experimental and numerical investigation for the flexural strengthening of RC beams using

near-surface mounted steel or GFRP bars. Constr Build Mater 2013;40: 145–61.
[45] Sharaky IA, Torres L, Comas J, Barris C. Flexural response of reinforced concrete (RC) beams strengthened with near surface mounted (NSM) fibre reinforced polymer (FRP) bars. Compos Struct 2014;109:8–22.
[46] Hognestad E. A study of combined bending and axial load in reinforced concrete members. University of Illinois Engineering Experiment Station, Bulletin no. 399.128; 1951.
[47] CEN. EN 1992-1-1:2004. Eurocode 2: Design of concrete structures - Part 1–1: General rules and rules for buildings. Eurocode 2; 2004.